Contents lists available at ScienceDirect

Computer Physics Communications
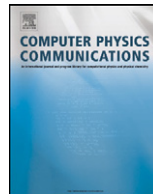
Spin stiffness of vector spin glasses

Frank Beyer [*], Martin Weigel

Institut für Physik, KOMET 331, Johannes Gutenberg-Universität Mainz, Staudinger Weg 7, 55128 Mainz, Germany

ARTICLE INFO	ABSTRACT
	We study domain-wall excitations for O(m) vector spin glasses in the limit $m \to \infty$, where the energy landscape is simplified considerably compared to XY or Heisenberg models due to the complete disappearance of metastability. Using numerical ground-state calculations and appropriate pairs of complementary boundary conditions, domain-wall defects are inserted into the systems and their excitation energies are measured. This allows us to determine the stiffness exponents for lattices of a range of spatial dimensions $d = 2, \ldots, 7$. Compiling these results, we can finally determine the lower critical dimension of the model. The outcome is compared to estimates resulting from field-theoretic calculations. © 2010 Elsevier B.V. All rights reserved.

1. Introduction

In view of the notorious difficulties in understanding the behavior of spin glass models of low spin dimension such as the Ising ($m = 1$), XY ($m = 2$) or Heisenberg ($m = 3$) models, it appears appealing to investigate the limiting case of vector spins with an infinite number of spin components ($m \to \infty$), which turns out to be simpler for analytical as well as numerical analyses. The model is described by the well-known Edwards–Anderson Hamiltonian

$$\mathcal{H} = -\frac{1}{2} \sum_{ij} J_{ij} \mathbf{S}_i \cdot \mathbf{S}_j, \qquad (1)$$

where the $\mathbf{S}_i \in \mathbb{R}^m$, $i = 1, \ldots, N$, are vector spins with m components, here taken to be normalized as $|\mathbf{S}_i| = 1$. The exchange couplings J_{ij} are drawn independently of each other from a Gaussian probability distribution with zero mean and unit standard deviation. The relative numerical ease of handling this limiting case is due to a significant simplification of the energy landscape with increasing spin dimension, namely a reduction in the number of metastable states. This effect also leads to an increase in the numerically accessible lattice sizes in MC simulations, e.g., of Heisenberg spin glasses [1] as compared to the Ising case [2].

Ising [2,3], and, to a lesser degree, XY [4] and Heisenberg [1, 5,6] models, have received most attention and it seems relatively clear now, that for all of them the lower critical dimension is $2 \leqslant d_l \leqslant 3$ [7], i.e., finite-temperature spin glass transitions are found in $d = 3$, but only zero-temperature transitions in $d = 2$. The situation is much less clear for general numbers m of spin components and, in particular, it is not ultimately known whether the lower critical dimension depends on the number of spin components for general m and in the limit of $m \to \infty$.

Considering a finite system of N spins in the limit of large spin dimensions, metastability vanishes completely and the ground state becomes unique, occupying only a finite-dimensional sub-manifold in spin space [8,9]. As a consequence, for each system size there exists a finite, critical number of spin components above which the ground-state energy does not change upon further adding spin dimensions, such that the system effectively describes a spherical spin glass, i.e. the limit $m \to \infty$. Compared to the field theoretic calculations [10,11], this corresponds to an interchange of the limits $N \to \infty$ and $m \to \infty$, such that the thermodynamic limit $N \to \infty$ is taken first in the perturbative calculations, whereas the infinite-component limit $m \to \infty$ is taken first in the numerical approach. This leads to some subtleties, such that the numerical approach might be considered the zeroth-order term in a $1/m$ expansion around the field-theoretic calculation [12].

There is a rigorous upper bound on the number of spin components beyond which no further change in the ground state is observed [9],

$$m_{\max}(N) = \lfloor (\sqrt{8N+1} - 1)/2 \rfloor \sim N^\mu, \quad \mu = 1/2, \qquad (2)$$

where $\lfloor x \rfloor$ stands for the largest integer smaller than or equal to x. For the fully connected or Sherrington–Kirkpatrick limit of the model, the average number of occupied spin dimensions in the ground state scales with an exponent $\mu = 2/5$ [8]. For the short-range, nearest-neighbor models on hyper-cubic lattices considered here, on the other hand, the spins require only a somewhat smaller number of spin components, with $\mu = \mu(d) < 2/5$ depending on the lattice dimension d [13]. This situation allows for the limit of an infinite number of spin components to be studied numerically for finite systems using only a finite number of spin components,

* Corresponding author.
E-mail address: beyerf@uni-mainz.de (F. Beyer).

Table 1
Parameters for the defect energy scaling with the P/AP setup for fits with different functional forms. Fits were performed for lattice sizes $L \geqslant L_{min}$.

d	$N_s/10^3$	aL^θ			$aL^\theta(1+b/L)$				$aL^\theta(1+b/L^2)$			
		L_{min}	θ	Q	L_{min}	θ	b	Q	L_{min}	θ	b	Q
2	3–5	5	−1.558(4)	0.76	4	−1.56(1)	−0.09(14)	0.76	4	−1.562(7)	−0.26(36)	0.77
3	3	7	−1.03(2)	0.99	3	−1.02(3)	0.21(22)	0.30	3	−1.03(2)	0.31(30)	0.30
4	3	6	−0.57(2)	0.23	3	−0.52(6)	0.51(44)	0.36	3	−0.57(3)	0.49(43)	0.31
5	10–18	7	−0.14(1)	0.97	4	−0.07(5)	0.64(39)	0.99	3	−0.11(1)	1.17(22)	0.99
6	5–13	5	0.27(2)	0.49	3	0.7(19)	5.0(380)	0.60	3	0.33(5)	1.60(55)	0.56
7	0.5	3	0.56(7)	0.98	–	–	–	–	–	–	–	–

for instance determining the lower critical dimension from defect-energy calculations. Previously reported results [13,14], however, did not reach up to the lattice dimensions above the apparent lower critical dimension, where an ordering effect would be expected at finite temperatures.

2. Ground state computations

Using the concept of the defect energy [15], we determined stiffness exponents for hypercubic lattices of spatial dimensions $d = 2, \ldots, 7$ and nearest-neighbor interactions. This widely-used approach in the study of spin-glass systems is based on the assumption that the cost ΔE of the insertion of a system-size defect into a state of the ordered phase scales as [16]

$$\Delta E \propto L^\theta, \tag{3}$$

where θ is known as the spin-stiffness exponent. The significance of θ is based on the observation that for $\theta < 0$ arbitrarily small thermal fluctuations suffice to destroy the ordered state in the thermodynamic limit, preventing a phase transition to occur at $T > 0$. On the contrary, $\theta > 0$ indicates the presence of a finite-temperature phase transition, since the cost of insertion of a system-size defect diverges in the thermodynamic limit, thus guaranteeing a stable ordered phase at sufficiently small (but non-zero) temperatures. If, to leading order, the defect energy remains constant, i.e. $\theta = 0$, the system is at its lower critical dimension d_l.

Calculation of defect energies with a numerical approach requires the determination of ground states for a set of different boundary conditions. Ground states were calculated here employing a local spin-quench procedure, for which the spins are iteratively aligned with their respective local molecular fields $\mathbf{H}_i$, as

$$\mathbf{S}_i' \parallel \mathbf{H}_i = \sum_{j \in \mathcal{N}(i)} J_{ij}\mathbf{S}_j, \tag{4}$$

where the sum runs over the set $\mathcal{N}(i)$ of nearest neighbors of the spin at site i. It is easily seen that alignment of each spin with its molecular field is a necessary condition for the system to be in its ground state. For the present case of a system without metastable states [8], it is also sufficient.

These updates are interspersed with sweeps of over-relaxation moves to speed up convergence, which have also been found to improve the decorrelation of systems with finite m in Monte Carlo simulations [5]. These moves, again being local, preserve the energy of the whole spin configuration since the updated spin is merely rotated around its local field and therefore moves at constant energy. The simplest way of implementing such a procedure, in particular for the case of arbitrary spin dimensions m, is to reflect the spin along $\mathbf{H}_i$, such that

$$\mathbf{S}_i' = -\mathbf{S}_i + 2\frac{\mathbf{S}_i \cdot \mathbf{H}_i}{|\mathbf{H}_i|^2}\mathbf{H}_i. \tag{5}$$

This maximal movement can also be argued to lead to a maximal decorrelation effect within the constant-energy manifold of single-spin movements. The whole procedure of spin-quench and over-relaxation moves can be implemented very efficiently, since only

a few elementary operations are required for each step, and no random numbers are involved.

Inducing a defect of linear size L, i.e., a domain wall, in the system can be accomplished by manipulating the boundaries in *one* lattice dimension. To reduce additional surface effects, boundary conditions in all other lattice directions were chosen periodic. Here, we decided to use three different setups aimed at reducing problems with domain walls trapped due to the periodicity and possibly discriminating between spin (rotational symmetry) and chiral [17] (discrete symmetry) defects [18]. Firstly, we investigated the case of periodic and anti-periodic (P/AP) boundary conditions as the standard setup to probe continuous or "spin" excitations. Since for this case domain walls might be trapped in *both* configurations due to the imposed periodicity, the difference between the two ground-state energies does not directly correspond to the excitation energy of a single defect [19,20]. To alleviate this problem, we also investigated open/domain-wall (O/DW) boundary conditions. In this case the defect energy is determined by comparing the energies of a system with open boundaries in one direction and a second one with fixed spins on two opposing boundaries, chosen to stay in the configuration found for open boundaries on one side and rotated around a common axis perpendicular to the hyperplane in spin space occupied by the boundary spins on the other side. Due to the open boundaries in the first case, the insertion of exactly one domain wall is guaranteed. A third type of boundary conditions (open/spin-pair) gave similar results compared to O/DW. These will be discussed elsewhere [21].

Previously, it was argued that corrections to scaling in defect energy studies are systematically reduced as systems of non-unit aspect ratio R are considered, i.e., lattices with geometry $L^{d-1} \times RL$, $R = 1, 2, \ldots$, which are elongated in one direction [22]. This appears to work quite well for Ising and XY systems that follow a well-defined power-law scaling in one dimension [20,22]. Due to an asymptotically *exponential* decay of defect energies with system size in the one-dimensional infinite-component limit [14], however, this approach appears to be of only limited applicability here [21]. Thus, instead of finding minimal corrections in the limit $R \to \infty$, best results are observed here for aspect ratios only moderately different from unity, and we chose $R = 2$ for the data discussed below as a compromise.

3. Results

Ground states were computed for a range of system sizes and the described sets of boundary conditions using between 3000 and 18 000 disorder realizations per lattice size, with more realizations used for the crucial cases with $|\theta|$ small. Due to the large computational effort, for $d = 7$ our data include only 500 disorder configurations. The number of disorder configurations N_s for each lattice dimension is indicated in Table 1. The resulting defect energies from P/AP boundary conditions for lattice dimensions $d = 2$, $d = 5$ and $d = 6$ are shown in Fig. 1. As is most clearly seen for the cases $d = 5$ and $d = 6$ with small $|\theta|$, corrections to the pure power-law behavior expected according to Eq. (3) are sizable and can be rather clearly resolved here due to the relatively large
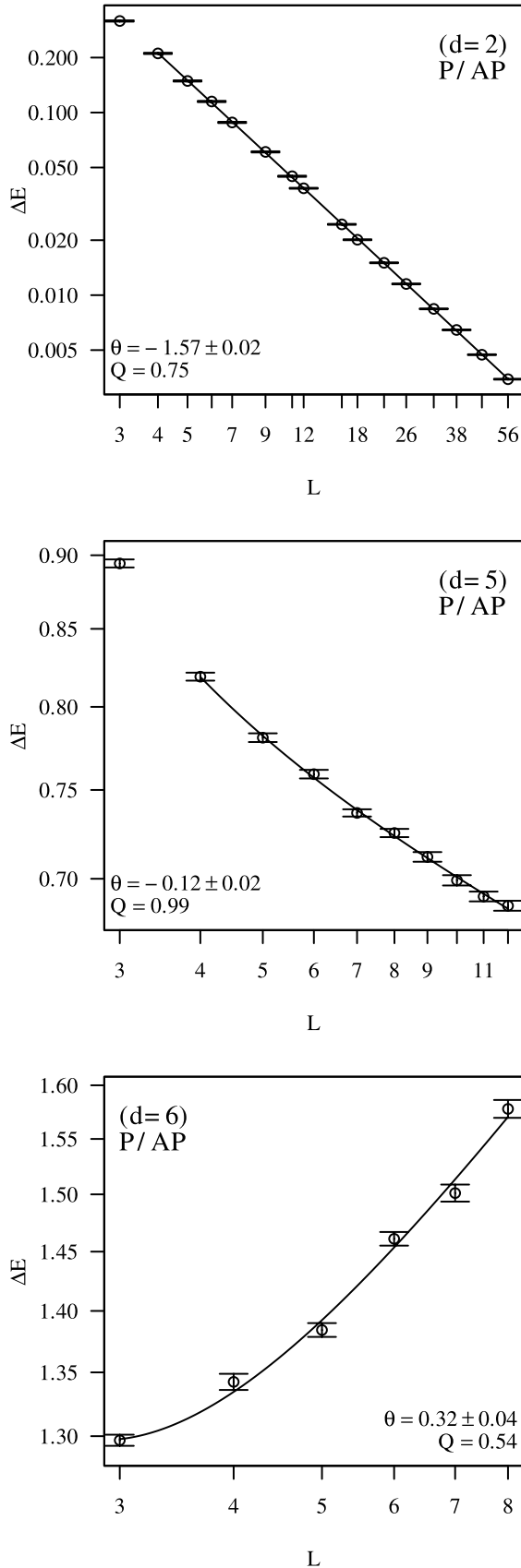
Fig. 1. Scaling of defect energies ΔE for P/AP boundary conditions with linear system size L in dimensions $d = 2$ (top), $d = 5$ (middle) and $d = 6$ (bottom). Between $d = 5$ and $d = 6$, the scaling exponent θ changes sign. Corrections to scaling around these dimensions are most pronounced. The lines are fits of the functional form (8) to the data.

Table 2
Parameters of fits of the functional form (8) to the data for P/AP boundaries.

d	L_{min}	$aL^\theta + b/L^2$		
		θ	b	Q
2	4	−1.57(2)	−0.21(36)	0.75
3	5	−0.99(6)	0.57(64)	0.29
4	4	−0.48(6)	1.31(61)	0.51
5	4	−0.12(2)	0.73(36)	0.99
6	3	0.32(4)	1.46(40)	0.54

number of disorder realizations. To describe these deviations, one might argue in favor of a correction resulting from a shift in the effective length scale,

$$\Delta E \sim a(L - L_0)^\theta = aL^\theta(1 - L_0/L)^\theta$$
$$= aL^\theta\left(1 + b/L + c/L^2 + \cdots\right). \tag{6}$$

Our data do not allow to resolve more than one correction term reliably, such that we have to restrict ourselves to including only the $1/L$ or only the $1/L^2$ term. Such fits, as monitored by the quality-of-fit parameter Q [23], work reasonably well, and the resulting estimates of θ are statistically compatible with those resulting from fits without correction terms, but omitting data points with $L < L_{min}$ for the smaller lattices, cf. the data collected in Table 1. Note the exception of the fit with $1/L$ correction term in $d = 6$ which leads to an estimate of θ way off the other estimates, indicating the statistical instability of the fit. For $d = 7$, the limited range of system sizes precludes the use of fits including correction terms. From the quality of the fits alone, we found it impossible to arrive at a general preference for either the $1/L$ or the $1/L^2$ form. Instead, we considered the effective form

$$\Delta E \sim aL^\theta\left(1 + bL^{-\omega}\right), \tag{7}$$

which resulted in parameters ω consistent with $\theta - \omega \approx 2$. We interpret these results in favor of a purely additive correction of the form

$$\Delta E \sim aL^\theta + b/L^2, \tag{8}$$

and, indeed, we find this form of fits to work well, cf. the fit results collected in Table 2. The corresponding fits are denoted by the solid lines in Fig. 1. The most relevant results are those for $d = 5$, where θ appears to be still slightly negative, and for $d = 6$, where our estimate of θ is positive. We might conclude, therefore, that the scaling character of defect energies changes in between and, consequently, $5 \leqslant d_l \leqslant 6$.

We now turn to the case of the O/DW setup of boundary conditions. Our corresponding results, averaged over the data for between 3000 and 5000 disorder realizations, are collected in Fig. 2. We find scaling corrections to be somewhat more pronounced here as compared to the P/AP setup, and they cannot fully be accounted for in all three lattice dimensions considered by either a $1/L$ correction or a $1/L^2$ correction term alone. We therefore used the effective description (7), which results in reasonable fits displayed in Fig. 2. The corresponding fit parameters are collected in Table 3. The rather low values of the quality-of-fit parameter Q in dimensions $d = 3$ and $d = 4$ are not a sign of general poor fit of the chosen functional form but, as closer inspection reveals, result from one or two outliers with relatively large deviations from the fit as compared to the (very small) statistical errors. Surprisingly, for the O/DW setup the spin-stiffness exponent θ changes sign already around $d = 3$, and it is clearly positive for the lattice dimensions $5 \leqslant d \leqslant 6$ where the crossover occurred for the P/AP boundaries.

One might wonder whether the apparently rather different estimates of stiffness exponents from the two boundary setups could
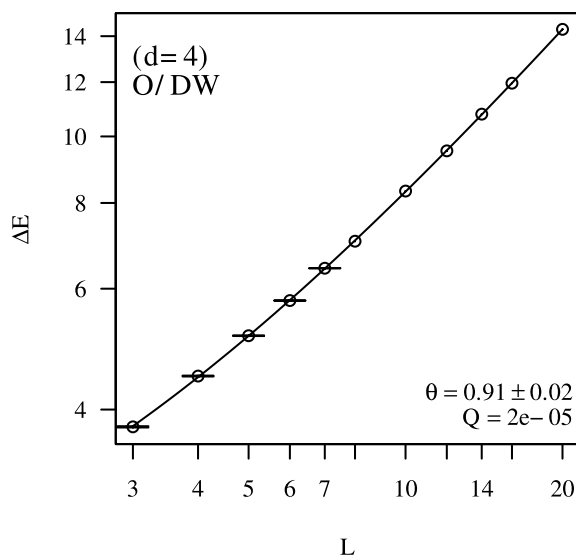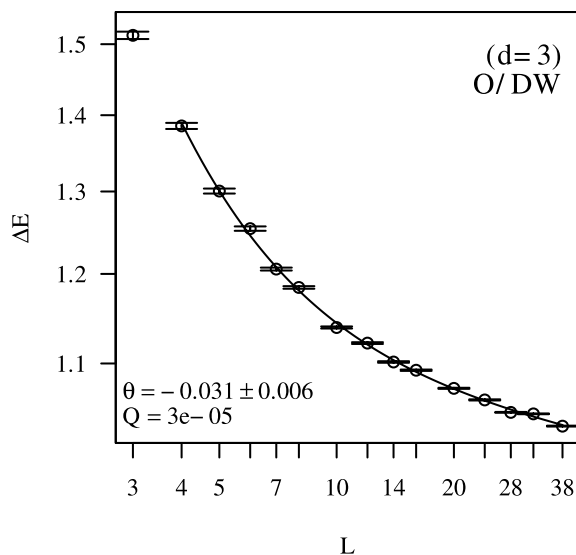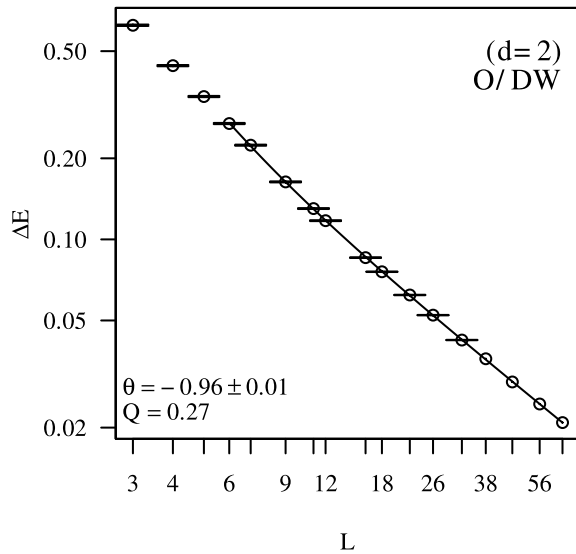
Fig. 2. Scaling of defect energies ΔE for O/DW boundary conditions with linear system size L in dimensions $d = 2$ (top), $d = 3$ (middle) and $d = 4$ (bottom) with fits of the functional form (7) to the data.
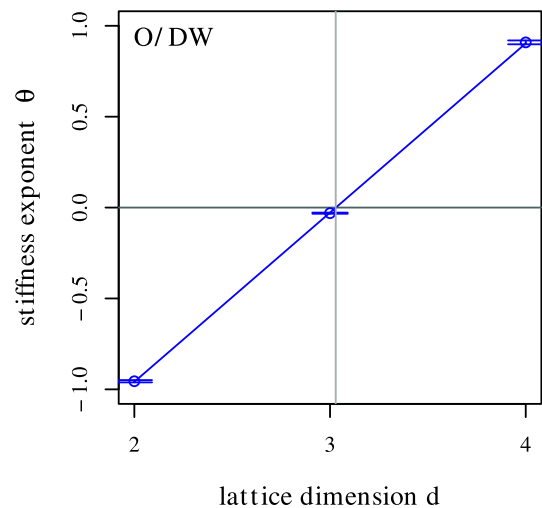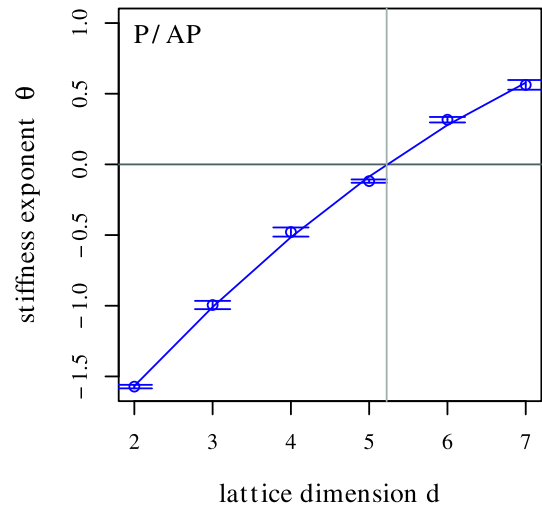
Fig. 3. Evolution of the spin stiffness exponent θ with lattice dimension d for P/AP boundary conditions (top) and for O/DW boundary conditions (bottom). The solid lines are guides to the eye.

be due to them exciting different types of defects, for instance of the spin and chiral character, respectively. While the O/DW construction certainly forms the cleaner setup in that one directly probes the energy of a single domain-wall defect, distinctions between spin and chiral excitations are subtle for this model: in general, we would associate the sign of the determinant of the considered O(m) rotation matrix with the chiral degrees of freedom [24]. For the chosen setup of boundaries, however, the determinant of the rotation matrix depends on whether the number of spin dimensions occupied by the boundary spins is even or odd. Since the required number of spin components fluctuates between disorder realizations, however, the chirality is formally maldefined after taking the disorder average. Also, we find no difference in scaling behavior between disorder realizations with even and those with odd spin dimensions. It appears more plausible, therefore, that the setup with O/DW boundaries implicitly probes the physically more realistic case of taking the $N \to \infty$ limit before the $m \to \infty$ limit where, from the experience with finite m, we expect a lower critical dimension $d \approx 3$. This possibility is the subject of extensions of the present work.

In view of our results for the two different setups of boundary conditions, summarized in Fig. 3, it would be desirable to also

Table 3
Parameters of fits of the functional form (7) to the data for O/DW boundaries.

d	$aL^\theta(1 + bL^{-\omega})$				
	L_{min}	θ	ω	b	Q
2	6	$-0.96(1)$	1.4(10)	4.7(16)	0.27
3	4	$-0.031(6)$	1.44(24)	1.94(27)	2.6×10^{-5}
4	3	0.91(2)	0.94(13)	1.803(35)	1.5×10^{-5}

study this model at finite temperatures, either by means of Monte Carlo simulations, or iterating equations derived from a saddle-point calculation as in Refs. [12,25]. The results of such calculations will be reported elsewhere [21]. As for now, the lower critical dimension of the model with $m \to \infty$ first appears to be $5 \leqslant d_l \leqslant 6$, consistent with the results of Ref. [10], but in contrast to the conjecture $d_l = 8$ of [11], based on a perturbation expansion. The upper critical dimension, on the other hand, is predicted to be 8 [10]. The alternative set of O/DW boundary conditions studied here might provide a means of studying the $m \to \infty$ limit of the finite-m models in the thermodynamic limit, for which one expects a lower critical dimension $d = 3$.

Acknowledgements

References

[1] D.X. Viet, H. Kawamura, Monte Carlo studies of chiral and spin ordering of the three-dimensional Heisenberg spin glass, Phys. Rev. B 80 (2009) 064418.

[2] M. Hasenbusch, A. Pelissetto, E. Vicari, Critical behavior of three-dimensional Ising spin glass models, Phys. Rev. B 78 (2008) 214205.

[3] H.G. Ballesteros, A. Cruz, L.A. Fernández, V. Martín-Mayor, J. Pech, J.J. Ruiz-Lorenzo, A. Tarancón, P. Téllez, C.L. Ullod, C. Ungil, Critical behavior of the three-dimensional Ising spin glass, Phys. Rev. B 62 (2000) 14237.

[4] J.H. Pixley, A.P. Young, Large-scale Monte Carlo simulations of the three-dimensional XY spin glass, Phys. Rev. B 78 (2008) 014419.

[5] I. Campos, M. Cotallo-Aban, V. Martín-Mayor, S. Perez-Gaviro, A. Tarancón, Spin-glass transition of the three-dimensional Heisenberg spin glass, Phys. Rev. Lett. 97 (2006) 217204.

[6] L.A. Fernández, V. Martín-Mayor, S. Perez-Gaviro, A. Tarancón, A.P. Young, Phase transition in the three dimensional Heisenberg spin glass: Finite-size scaling analysis, Phys. Rev. B 80 (2009) 024422.

[7] N. Kawashima, H. Rieger, Recent progress in spin glasses, in: H.T. Diep (Ed.), Frustrated Spin Systems, World Scientific, Singapore, 2004, pp. 491–596.

[8] M. Hastings, Ground state and spin-glass phase of the large-n infinite-range spin glass via supersymmetry, J. Stat. Phys. 99 (2000) 171–217.

[9] S. Chandra, Dependence of ground-state energy of classical n-vector spins on n, Phys. Rev. E 77 (2008) 021125.

[10] J.E. Green, A.J. Bray, M.A. Moore, Critical behaviour of an m-vector spin glass for $m = \infty$, J. Phys. A 15 (1982) 2307–2314.

[11] L. Viana, Infinite-component spin-glass model in the low-temperature phase, J. Phys. A 21 (1988) 803–813.

[12] L.W. Lee, A. Dhar, A.P. Young, Spin glasses in the limit of an infinite number of spin components, Phys. Rev. E 71 (2005) 036146.

[13] L. Lee, A. Young, Defect energy of infinite-component vector spin glasses, Phys. Rev. E 72 (2005) 036124.

[14] B. Morris, S. Colborne, M. Moore, A. Bray, J. Canisius, Zero-temperature critical behaviour of vector spin glasses, J. Phys. C 19 (1986) 1157–1171.

[15] J.R. Banavar, M. Cieplak, Nature of ordering in spin-glasses, Phys. Rev. Lett. 48 (1982) 832–835.

[16] A.J. Bray, M.A. Moore, Lower critical dimension of Ising spin glasses: a numerical study, J. Phys. C 17 (1984) L463–L468.

[17] J. Villain, Two-level systems in a spin-glass model: I. General formalism and two-dimensional model, J. Phys. C 10 (1977) 4793–4803.

[18] M. Weigel, M. Gingras, Ground states and defect energies of the two-dimensional XY spin glass from a quasiexact algorithm, Phys. Rev. Lett. 96 (2006) 097206.

[19] J.M. Kosterlitz, N. Akino, Numerical study of spin and chiral order in a two-dimensional XY spin glass, Phys. Rev. Lett. 82 (1999) 4094–4097.

[20] M. Weigel, M.J.P. Gingras, Zero-temperature phase of the XY spin glass in two dimensions: Genetic embedded matching heuristic, Phys. Rev. B 77 (2008) 104437.

[21] F. Beyer, M. Weigel, in preparation.

[22] A.C. Carter, A.J. Bray, M.A. Moore, Aspect-ratio scaling and the stiffness exponent θ for Ising spin glasses, Phys. Rev. Lett. 88 (2002) 077201.

[23] S. Brandt, Data Analysis: Statistical and Computational Methods for Scientists and Engineers, Springer, Berlin, 1998.

[24] H. Kawamura, Generalized chiral universality, J. Phys. Soc. Jpn. 59 (1990) 2305–2308.

[25] T. Aspelmeier, M.A. Moore, Generalized Bose–Einstein phase transition in large-m component spin glasses, Phys. Rev. Lett. 92 (2004) 077201.